The Astrophysical Journal Letters, 821:L20 (5pp), 2016 April 20 doi:10.3847/2041-8205/821/2/L20

THE FIRST DETECTION OF GeV EMISSION FROM AN ULTRALUMINOUS INFRARED GALAXY: Arp 220 AS SEEN WITH THE *FERMI* LARGE AREA TELESCOPE

Fang-Kun Peng[1,2], Xiang-Yu Wang[1,2], Ruo-Yu Liu[3], Qing-Wen Tang[4], and Jun-Feng Wang[5]
[1] School of Astronomy and Space Science, Nanjing University, Nanjing 210093, China; xywang@nju.edu.cn
[2] Key Laboratory of Modern Astronomy and Astrophysics (Nanjing University), Ministry of Education, Nanjing 210093, China
[3] Max-Planck-Institut für Kernphysik, D-69117 Heidelberg, Germany
[4] School of Science, Nanchang University, Nanchang 330031, China
[5] Department of Astronomy and Institute of Theoretical Physics and Astrophysics, Xiamen University, Xiamen, Fujian 361005, China
Received 2016 March 21; accepted 2016 April 1; published 2016 April 14

ABSTRACT

Cosmic rays (CRs) in starburst galaxies produce high-energy gamma-rays by colliding with the dense interstellar medium. Arp 220 is the nearest ultraluminous infrared galaxy that has star formation at extreme levels, so it has long been predicted to emit high-energy gamma-rays. However, no evidence of gamma-ray emission was found despite intense search efforts. Here we report the discovery of high-energy gamma-ray emission above 200 MeV from Arp 220 at a confidence level of $\sim 6.3\sigma$ using 7.5 years of *Fermi* Large Area Telescope observations. The gamma-ray emission shows no significant variability over the observation period and it is consistent with the quasi-linear scaling relation between the gamma-ray luminosity and total infrared luminosity for star-forming galaxies, suggesting that these gamma-rays arise from CR interactions. As the high-density medium of Arp 220 makes it an ideal CR calorimeter, the gamma-ray luminosity can be used to measure the efficiency of powering CRs by supernova (SN) remnants given a known supernova rate in Arp 220. We find that this efficiency is about $4.2 \pm 2.6\%$ for CRs above 1 GeV.

Key words: gamma-rays: galaxies – galaxies: starburst – cosmic rays

1. INTRODUCTION

Nearby star-forming and starburst galaxies have been identified to be GeV to TeV gamma-ray sources (Acero et al. 2009; VERITAS Collaboration et al. 2009; Abdo et al. 2010; Ackermann et al. 2012). Cosmic rays (CRs) accelerated by supernova remnants interact with the interstellar gas and produce neutral pions (schematically written as $p + p \rightarrow \pi^0 +$ other products), which in turn decay into high-energy gamma-rays ($\pi^0 \rightarrow \gamma + \gamma$). High energy gamma-ray emission is thus a powerful tool to diagnose the non-thermal emission related with CRs in star-forming galaxies.

Arp 220, at a distance of $d = 77$ Mpc, is the nearest ultraluminous infrared galaxy (ULIRG), with a total infrared luminosity of $(1\text{–}2) \times 10^{12} L_{\odot}$ (Sanders et al. 2003; Gao & Solomon 2004; Rangwala et al. 2011). The system is a merger of two galaxies and contains two dense nuclei separated by 350 pc. Both nuclei have high star formation rates and dense molecular gas. Arp 220 has a molecular gas mass of $10^{10} M_{\odot}$ (Scoville et al. 1997) and a total star formation rate of $240 \pm 30\, M_{\odot}\, \mathrm{yr}^{-1}$, calculated with the far-infrared luminosity (Farrah et al. 2003). Radio detection of supernovae suggests a high rate of $4 \pm 2\, \mathrm{yr}^{-1}$ (Smith et al. 1998; Lonsdale et al. 2006; Parra et al. 2007). Although Arp 220 could contain active galactic nuclei (AGNs) (Paggi et al. 2013; Teng et al. 2015), the observed high supernova rate indicates that star formation provides a substantial fraction of the power radiated by the nuclei.

As a huge reservoir of molecular gas, the nuclei of Arp 220 should be complete proton calorimeters, i.e., the CR protons lose all of their energy to secondary pions via collisions with the gases before escaping (Torres 2004; Thompson et al. 2007; Lacki et al. 2011; Yoast-Hull et al. 2015). Given a high CR emissivity and a high efficiency of converting CR energy into gamma-rays, Arp 220 was predicted to emit GeV to TeV gamma-rays (Torres 2004; Lacki et al. 2011; Yoast-Hull et al. 2015). There have been intense efforts to search for GeV emission from Arp 220 (Lacki et al. 2011; Ackermann et al. 2012; Tang et al. 2014). Tang et al. (2014) obtained an upper limit of $F_{0.1-100\ \mathrm{GeV}} < 3.5 \times 10^{-9}\ \mathrm{ph\ cm^{-2}\ s^{-1}}$ at the 95% confidence level using 68 months of *Fermi*/LAT data. Arp 220 was also observed by the VERITAS telescopes at TeV energies for more than 30 hr, but no significant excess over the background was found (Fleischhack et al. 2015). Here we report the detection of GeV emission from Arp 220 using 7.5 years of *Fermi*/LAT data reprocessed with Pass 8, the newest event-level analysis, which significantly improves the acceptance and angular resolution of the instrument.[6]

We present a description of the analysis and show the results in Section 2. Then we discuss the origin of the γ-ray emission in Section 3 and use it to constrain the CR acceleration efficiency in Section 4. Finally we give the conclusions in Section 5.

2. DATA ANALYSIS

2.1. Data Selection

We choose the *Fermi*/LAT survey data with the P8R2 SOURCE event class from 2008 August 04 to 2016 January 22, and use the current *Fermi* science tools version v10r0p5 for data analysis (Atwood et al. 2009). A maximum zenith angle of $<90^{\circ}$ is selected to reduce the Earth Limb emission. The data are filtered with the recommended cuts (DATA_QUAL > 1) & (LAT_CONFIG $== 1$) & ABS(ROCK_ANGLE) $< 52^{\circ}$. Photons with energy ranging between 200 MeV and 100 GeV are taken into consideration. The region of interest (ROI) is a circle with a radius of 10° centered at the position of Arp 220 (i.e., R.A. $= 233^{\circ}.738$, decl. $= 23^{\circ}.5032$, J2000). We use the

[6] http://fermi.gsfc.nasa.gov/ssc/

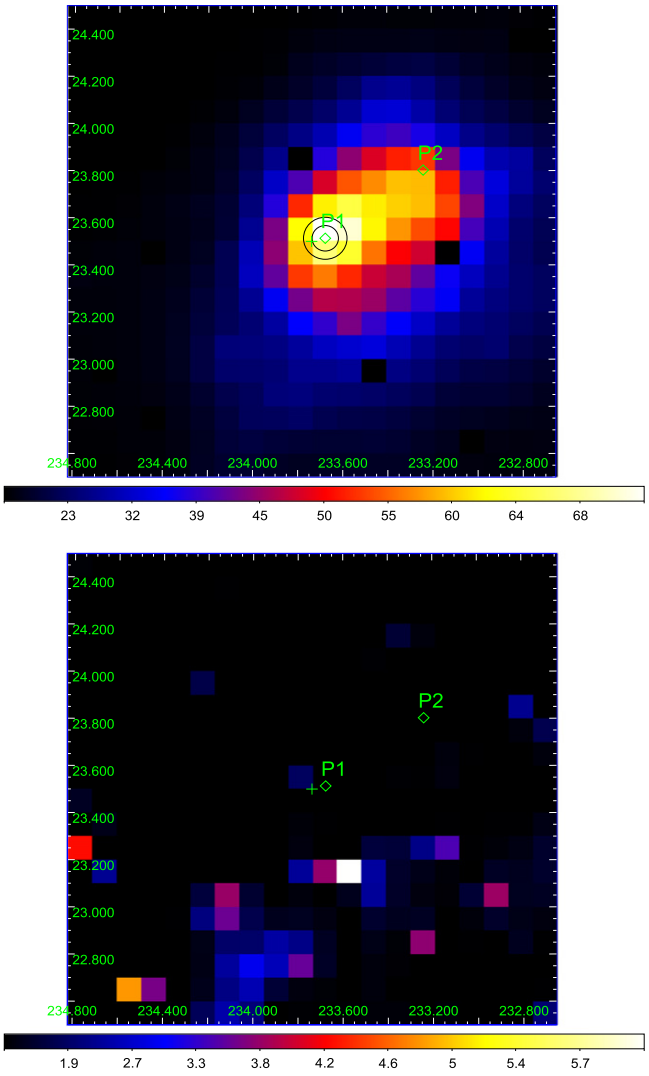

Figure 1. TS map with bin size = 0.°1 above 200 MeV for the 2° × 2° region centered at Arp 220 (R.A., decl. = 233.°738, 23.°5032). The green cross denotes the position of Arp 220, and the black lines show the 1σ and 2σ errors around P1. The green diamonds denote the positions of P1 and P2. The upper panel shows the residual TS map after removing the emission from 3FGL point sources, the galactic diffuse emission, and isotropic emission. The bottom panel shows the residual TS map after removing emissions farther from P1 and P2.

FRONT+BACK converting photons. The 3FGL sources (Acero et al. 2015) within 15° of the ROI center are included in the source model. The galactic diffuse emission and isotropic emission are respectively modeled with "gll_iem_v06.fits" and "iso_P8R2_SOURCE_V6_v06.txt". We also consider the CLEAN data and binned method to check our results and no statistical difference is found.

2.2. Spatial and Spectral Analysis

We start with a preliminary unbinned likelihood analysis on the ROI with the tool *gtlike*, only including "gll_iem_v06.fits," "iso_P8R2_SOURCE_V6_v06.txt" and point sources of 3FGL within 15° from the ROI center in the source model file. The residual test-statistic (TS) under this scenario is shown in the upper panel of Figure 1, which shows a gamma-ray excess around Arp 220. We add one point source with a power-law spectrum at the local maxima of the TS map in the source model file. We re-fit the data and find the best-fit γ-ray emission position with the tool *gtfindsrc*. We then change the position of the point source to the obtained best-fit location of γ-ray emission in the source model file. Repeating the standard analysis threads and computing the TS map, although we find a significantly improved fit, we note that there is still some residual emission to the northwest of the ROI center. In order to explore the high-energy emission more accurately near Arp 220 and reduce the contamination from nearby background sources, a second point source is added to the source model based on the residual γ-ray emission. By utilizing the tool *gtfindsrc*, we optimize the position of these two point sources, namely P1 (233.°677, 23.°5163) ± 0.°054, which is near Arp 220 and P2 (233.°239, 23.°8049) ± 0.°168, which is located at a position about 0.°5 away from Arp 220, as marked in Figure 1. Next, we re-fit the data with point sources P1 and P2 in the source model file, and get a better result with Δ likelihood = 8 (i.e., we get a global improved fitting with significance TS = 16), in comparison with only one point source being added into the source model file. The significance of $TS_{P2} = 22$ suggests that P2 should be a genuine additional γ-ray source. The bottom panel in Figure 1 illustrates that there is little residual γ-ray emission near the vicinity of Arp 220 region. The source model file including point sources P1 and P2 will be used in all the subsequent analysis.

We now check possible alternative candidates for P1 and P2 in the following catalogs: the CRATES Flat-Spectrum Radio Source Catalog (Healey et al. 2007), the Veron Catalog of Quasars AGN, the 13th Edition (Véron-Cetty & Véron 2010), and the Candidate Gamma-Ray Blazar Survey Source Catalog (Healey et al. 2008). No other sources are found in the vicinity of r_{95} of P1 except for Arp 220. With only a separation of 0.°058 between P1 and Arp 220, it is reasonable to ascribe the high-energy emission from P1 to Arp 220. In contrast, the separation between P2 and Arp 220 reaches 0.°547 and there are four candidates around r_{95} of P2 in the above three catalogs: CRATES J153246+234400 (4.′902), an FSRQ with unknown redshift; SDSS J15323+2345 (9.′080), a QSO with redshift $z = 1.465$; SDSS J15337+2358 (14.′643), a Seyfert 1 galaxy with $z = 0.067$; and 1WGA J1533.8+2356 (15.′315), an AGN of unknown type located at $z = 0.232$. The values in the parentheses are the angular offsets of these sources from P2. We suspect that the gamma-ray emission from P2 is contributed by one or more of these AGNs.

We assume power-law spectra in the range of 0.2–100 GeV for both P1 and P2 in the aforementioned best source model files. The best-fit photon index for emissions of P1 is $\Gamma_1 = 2.35 \pm 0.16$ with a total flux of $F_1 = 1.76 \pm 0.52 \times 10^{-9}$ ph cm^{-2} s^{-1}. Regarding P2, the photon index is $\Gamma_2 = 2.45 \pm 0.19$ and the total flux is $F_2 = 1.45 \pm 0.52 \times 10^{-9}$ ph cm^{-2} s^{-1}. The corresponding energy fluxes in 0.2–100 GeV are $1.92 \pm 0.43 \times 10^{-12}$ erg cm^{-2} s^{-1} and $1.39 \pm 0.40 \times 10^{-12}$ erg cm^{-2} s^{-1} for P1 and P2, respectively. The spatial and spectral results of P1 and P2 are summarized in Table 1. The spectral energy distribution (SED) of P1 (Arp 220) is shown in Figure 2. We do not discuss P2 further in this paper since our focus is on the gamma-ray emission from Arp 220.

3. ORIGIN OF THE GAMMA-RAY EMISSION FROM ARP 220

Gamma-ray emissions in star-forming galaxies are usually thought to originate from CR protons via collision with the

Table 1
The Best-fit Spectral Parameters of the Point Sources around the Arp 220 Region for Energy Band 0.2–100 GeV

Point	Position (degree)	r_{95} (degree)	Separation (degree)	Photon Flux (10^{-9} ph cm^{-2} s^{-1})	Energy Flux (10^{-12} erg cm^{-2} s^{-1})	Γ	TS	Association
P1	(233.677, 23.5163)	0.090	0.058	1.76 ± 0.52	1.92 ± 0.43	2.35 ± 0.16	40	Arp 220
P2	(233.239, 23.8049)	0.279	0.547	1.45 ± 0.52	1.39 ± 0.40	2.45 ± 0.19	22	···

Note. The fourth column is the angle distance between the best-fit position of γ-ray excess and the position of Arp 220.

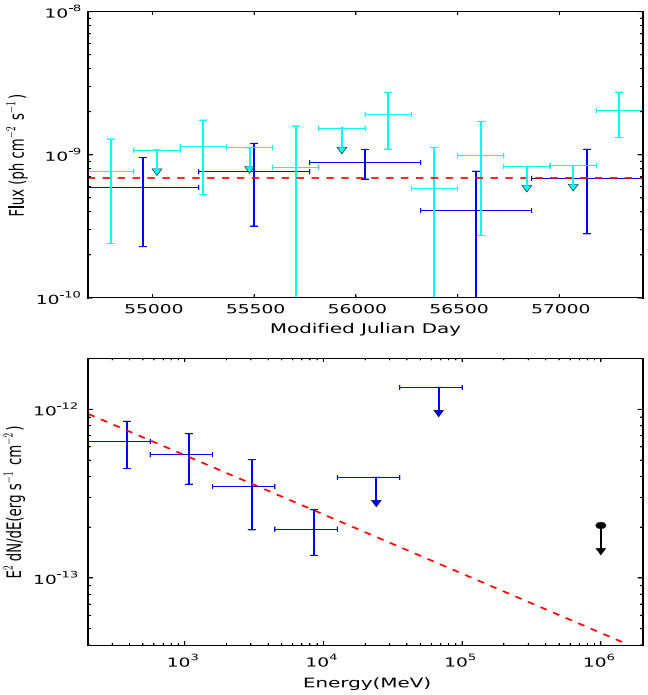

Figure 2. Upper panel: *Fermi*/LAT (0.4–100 GeV) light curves of P1 (Arp 220). The blue (cyan) data points indicate the light curve for five (twelve) time bins. The red dashed line illustrates the maximum likelihood flux level for the ∼7.5 year observations. Bottom panel: The spectral energy distribution of P1 (Arp 220). The upper limits of two blue data points are at the 95% confidence level. The red dashed line illustrates the best-fit power-law spectral model in 0.2–100 GeV with the unbinned analysis. The black data point is derived from the integral upper limit flux observed by VERITAS (Fleischhack et al. 2015).

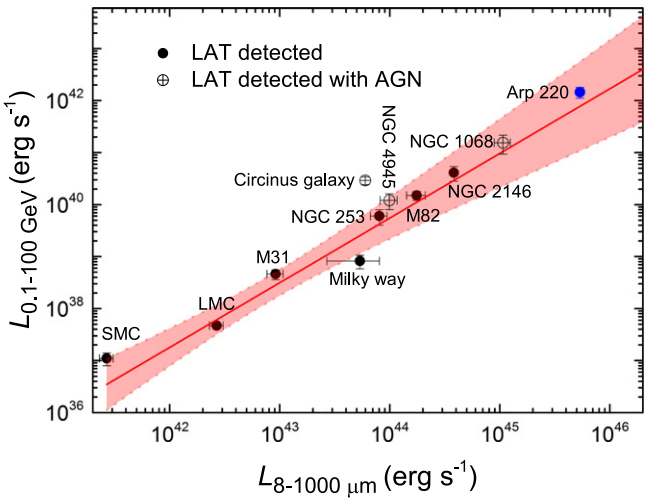

Figure 3. Gamma-ray luminosity (0.1–100 GeV) vs. total infrared luminosity (8–1000 μm) for LAT-detected star-forming galaxies and Seyferts. The red solid line is the best-fit power-law relation for star-forming galaxies only (black filled circles). Two dotted lines represent its 95% confidence level region around the best fit. Arp 220, marked with the blue filled circle, lies on the extrapolation of this relation to higher luminosity. The total infrared luminosity data are taken from Gao & Solomon (2004), and γ-ray luminosities are taken from Ackermann et al. (2012) and Tang et al. (2014).

gases inside the galaxies. This may especially be the case with Arp 220, as it has a high supernova rate and high gas density. Alternatively, Arp 220 could have hidden AGNs (Paggi et al. 2013; Teng et al. 2015), which in principle could give rise to gamma-ray emission as well. CR-induced gamma-ray emission in a star-forming galaxy is expected to be stable, while gamma-ray emission induced by AGNs should be temporally variable (Gasparrini et al. 2015). Thus, we examine the flux variability of Arp 220 (P1). We create a set of time bins for the light curve of photons with energy >400 MeV. In the first trial, the full observation period is divided linearly into five equal time bins. Each time bin is fitted by a separate maximum likelihood analysis, resulting in each bin having a detection significance TS > 4. We further check a finer light curve with 12 time bins. The χ^2 goodness-of-fit test is consistent with a constant flux with a reduced χ^2 of 0.83 for data points with a detection significance TS > 1. The results are shown in Figure 2. None of the two cases show significant changes in flux over the period of LAT observations.[7] Generally speaking, the temporal behavior of GeV emission from Arp 220 resembles that of other starburst galaxies, such as M82 and NGC 253.

Meanwhile, there is a clear positive empirical relation between the γ-ray luminosity $L_{0.1-100\ \mathrm{GeV}}$ and total infrared luminosity $L_{8-1000\ \mu\mathrm{m}}$ in local group galaxies and nearby star-forming galaxies[8](Ackermann et al. 2012). With a pure sample of star-forming galaxies, Tang et al. (2014) have drawn a similar relation and extended the relation to a luminous infrared galaxy NGC 2146. The best simple linear fit for nearby star-forming galaxies excluding Arp 220 gives a relation of

$$\log\left(\frac{L_{0.1-100\ \mathrm{GeV}}}{\mathrm{erg\ s^{-1}}}\right) = \alpha + \beta\log\left(\frac{L_{8-1000\ \mu\mathrm{m}}}{\mathrm{erg\ s^{-1}}}\right). \quad (1)$$

(see Figure 3), where $\alpha = -14.98 \pm 4.87$ and $\beta = 1.24 \pm 0.11$ are the intercept and slope, respectively. The Pearson's correlation coefficient is 0.98, with a chance probability of $p \sim 10^{-4}$. With a luminosity of $L_{0.1-100\ \mathrm{GeV}} = 1.78 \pm 0.30 \times 10^{42}$ erg s^{-1}, Arp 220 is consistent

[7] The gamma-ray excess indicated by the P7 data in Tang et al. (2014) is located at a position within r_{95} of P2, so this excess has nothing to do with Arp 220 (P1). The source of this gamma-ray excess in Tang et al. (2014) was likely FSRQ CRATES J153246+234400, which shows variability.

[8] Although the origins of the high-energy emission of two starbursting Seyfert 2 galaxies NGC 1068 and NGC 4945 are not yet definitely established, the lack of γ-ray variability and the consistent behavior with this correlation favor a CR origin.

with this quasi-linear relation. It is also consistent with the scaling relation between the gamma-ray luminosity and radio luminosity found for star-forming galaxies (Ackermann et al. 2012). The fact that the gamma-ray emission has no significant variability over the observation period and it is consistent with the above scaling relation suggests that the gamma-ray emission is likely to arise from CR interactions.

4. MEASURING THE CR ACCELERATION EFFICIENCY

As the ejecta of a SN encounter the ambient interstellar medium (ISM), a strong shock will be generated and a fraction of the kinetic energy of the ejecta will be transferred into CRs. The gamma-ray luminosity of a galaxy depends on both the efficiency of converting SN kinetic energy to CRs and the efficiency of converting CR energy to gamma-rays (i.e., the proton–proton collision efficiency). Because of the very dense ISM in Arp 220, it has been widely suggested that Arp 220 is an ideal proton calorimeter, since the collisional energy loss time of CR protons is much shorter than the time that CRs escape out of the galaxy (Lacki et al. 2011; Yoast-Hull et al. 2015). Then its gamma-ray luminosity provides a direct tool to measure the efficiency that SN explosion power goes into high-energy CRs.

Assuming that SNRs are the sole source of CR protons, and that a constant fraction (η) of SN kinetic energy is transferred into CR protons with energy above 1 GeV, the total injected CR power reads

$$L_{\rm CR}(>1\ {\rm GeV}) = 1.3\times10^{44}\ {\rm erg\ s^{-1}} E_{51}\eta\left(\frac{\Gamma_{\rm SN}}{4\ {\rm yr^{-1}}}\right), \quad (2)$$

where E is the SN kinetic energy, which is typically 10^{51} erg, and $\Gamma_{\rm SN}=4\pm2\,{\rm yr^{-1}}$ is the SN rate obtained by the radio observations (Smith et al. 1998; Lonsdale et al. 2006; Parra et al. 2007). On the other hand, by assuming that the system reaches a steady state, one can derive the injected CR power from the observed gamma-ray luminosity. As leptonic emission is expected to become increasingly important at lower energies, contaminating the estimate of the power in CR protons, we only consider the γ-ray emission above 1 GeV. Then we have

$$L_{\rm CR}(>1\ {\rm GeV}) = 3L_\gamma(>1\ {\rm GeV})(\Gamma-1)\beta_\pi^{-1}. \quad (3)$$

Here the prefactor 3 is due to that only 1/3 of the lost CR power goes into gamma-rays, as inelastic proton–proton collisions produce both neutral and charged pions. The factor $\Gamma-1$ arises from the fact that a fraction $(\Gamma-2)/(\Gamma-1)$ of the energy of CRs above 1 GeV is transferred to lower energy CRs, where Γ is the CR spectral index, which is equal to the photon index of the gamma-ray emission in our case. Since not all the pionic gamma-rays produced by CRs will have energies above 1 GeV, we need another correction factor $\beta_\pi\simeq0.6$ (for $\Gamma=-2.35$) to account for this effect (Lacki et al. 2011). Given that the luminosity of Arp 220 above 1 GeV is $L_\gamma(>1\ {\rm GeV})=(0.75\pm0.28)\times10^{42}\,{\rm erg\,s^{-1}}$, we can obtain the CR acceleration efficiency from Equations (2) and (3), i.e.,

$$\eta\simeq(4.2\pm2.6)\%E_{51}^{-1}\left(\frac{\beta_\pi}{0.6}\right)^{-1}\left(\frac{\Gamma_{\rm SN}}{4\ {\rm yr^{-1}}}\right)^{-1}. \quad (4)$$

Note that here only the uncertainties in $\Gamma_{\rm SN}$ and $L_\gamma(>1\ {\rm GeV})$ are taken into consideration to estimate the uncertainty in η. To our knowledge, this is the first time that such an efficiency has been obtained directly from gamma-ray observations. The obtained efficiency in Arp 220 is consistent with estimates of a 3%–10% efficiency in the Milky Way (Strong et al. 2010) and a 6% efficiency in NGC 253 and M82 (Paglione & Abrahams 2012).

5. CONCLUSIONS

Through the analysis of 7.5 years of *Fermi*/LAT observations, we find high-energy gamma-ray emission above 200 MeV from Arp 220 with a detection significance of about 6.3σ. This is the first time that GeV emission has been detected from an ULIRG. The reconstructed energy spectrum is best modeled by a single power law with a photon index $\Gamma=2.35\pm0.16$ and the integrated flux in 0.2–100 GeV is $F_{0.2-100\ {\rm GeV}}=(1.76\pm0.52)\times10^{-9}\,{\rm ph\,cm^{-2}\,s^{-1}}$. The fact that no evidence of significant variability is found and that the gamma-ray emission is consistent with some scaling relations for star-forming galaxies implies that the gamma-ray emission of Arp 220 is likely from CR-induced diffuse emission. As Arp 220 is an ideal proton calorimeter, the gamma-ray luminosity can be used to directly measure the CR acceleration efficiency by SNRs, which gives an efficiency of $4.2\pm2.6\%$ for CRs above 1 GeV.

We thank Anton Prosekin and Gwenael Giacinti for useful discussions and the anonymous referee for a helpful report. This work has made use of data and software provided by the *Fermi* Science Support Center. It has also made use of the NASA/IPAC Extragalactic Database (NED) which is operated by the Jet Propulsion Laboratory, California Institute of Technology, under contract with the National Aeronautics and Space Administration. This work is supported by the 973 program under grant 2014CB845800, the NSFC under grants 11273016 and 11033002, and the Excellent Youth Foundation of Jiangsu Province (BK2012011). J.W. acknowledges support from NSFC grant 11473021 and the Fundamental Research Funds for the Central Universities under grants 20720150168 and 20720160023.

REFERENCES

Abdo, A. A., Ackermann, M., Ajello, M., et al. 2010, ApJL, 709, L152
Acero, F., Ackermann, M., Ajello, M., et al. 2015, ApJS, 218, 23
Acero, F., Aharonian, F., Akhperjanian, A. G., et al. 2009, Sci, 326, 1080
Ackermann, M., Ajello, M., Allafort, A., et al. 2012, ApJ, 755, 164
Atwood, W. B., Abdo, A. A., Ackermann, M., et al. 2009, ApJ, 697, 1071
Farrah, D., Afonso, J., Efstathiou, A., et al. 2003, MNRAS, 343, 585
Fleischhack, H., et al. (for the VERITAS Collaboration) 2015, arXiv:1508.05807
Gao, Y., & Solomon, P. M. 2004, ApJ, 606, 271
Gasparrini, D., Lott, B., Cutini, S., Ciprini, S. & Elisabetta Cavazzuti (for the Fermi LAT Collaboration) 2015, arXiv:1508.05301
Healey, S. E., Romani, R. W., Cotter, G., et al. 2008, ApJS, 175, 97
Healey, S. E., Romani, R. W., Taylor, G. B., et al. 2007, ApJS, 171, 61
Lacki, B. C., Thompson, T. A., Quataert, E., Loeb, A., & Waxman, E. 2011, ApJ, 734, 107
Lonsdale, C. J., Diamond, P. J., Thrall, H., Smith, H. E., & Lonsdale, C. J. 2006, ApJ, 647, 185
Paggi, A., Fabbiano, G., Risaliti, G., Wang, J., & Elvis, M. 2013, ApJ, submitted (arXiv:1303.2630)
Paglione, T. A. D., & Abrahams, R. D. 2012, ApJ, 755, 106
Parra, R., Conway, J. E., Diamond, P. J., et al. 2007, ApJ, 659, 314

Rangwala, N., Maloney, P. R., Glenn, J., et al. 2011, ApJ, 743, 94
Sanders, D. B., Mazzarella, J. M., Kim, D.-C., Surace, J. A., & Soifer, B. T. 2003, AJ, 126, 1607
Scoville, N. Z., Yun, M. S., & Bryant, P. M. 1997, ApJ, 484, 702
Smith, H. E., Lonsdale, C. J., Lonsdale, C. J., & Diamond, P. J. 1998, ApJL, 493, L17
Strong, A. W., Porter, T. A., Digel, S. W., et al. 2010, ApJL, 722, L58
Tang, Q.-W., Wang, X.-Y., & Tam, P.-H. T. 2014, ApJ, 794, 26
Teng, S. H., Rigby, J. R., Stern, D., et al. 2015, ApJ, 814, 56
Thompson, T. A., Quataert, E., & Waxman, E. 2007, ApJ, 654, 219
Torres, D. F. 2004, ApJ, 617, 966
Véron-Cetty, M.-P., & Véron, P. 2010, A&A, 518, A10
VERITAS Collaboration, Acciari, V. A., Aliu, E., et al. 2009, Natur, 462, 770
Yoast-Hull, T. M., Gallagher, J. S., & Zweibel, E. G. 2015, MNRAS, 453, 222